Metabolite release and rheological properties of sponge cake after *in vitro* digestion and the influence of a flour replacer rich in dietary fibre

Min Huang [a,b], Xue Zhao [a,b], Yihan Mao [a], Lin Chen [a,b], Hongshun Yang [a,b,*]

[a] *Department of Food Science and Technology, National University of Singapore, Singapore 117543, Singapore*
[b] *National University of Singapore (Suzhou) Research Institute, 377 Lin Quan Street, Suzhou Industrial Park, Suzhou, Jiangsu 215123, PR China*

ABSTRACT

The present study aimed to better understand the metabolite release and rheological characteristics of sponge cake after *in vitro* digestion and the effect of *Eucheuma* as a fibre-rich flour replacer. Overall, 22 compounds including amino acids, saccharides, fatty acids, and other metabolites were identified based on nuclear magnetic resonance spectra. Principal component analysis and orthogonal projection to latent structures-discriminant analysis showed that *Eucheuma* reduced the release of amino acids and fatty acids. The released glucose from the EP20 sample (20% replacement of flour with *Eucheuma*) decreased by 35.4% in intestinal phases compared with the control cake. *Eucheuma*'s *in vitro* effects on sponge cake digestion mainly reflected altered flow behaviour index. All samples showed solid–like behaviour and a decrease in viscoelastic moduli after digestion. This study forms the basis for future optimisation of food properties to control their digestive characteristics.

1. Introduction

The estimation of food digestion processes has been studied intensively using *in vitro* digestion models (Diez-Sánchez et al., 2018; Marcano et al., 2015). The *in vitro* digestion models can imitate the *in vivo* physiological conditions, including the species and concentrations of digestive enzymes, salt concentrations, pH conditions, and digestion time (Minekus et al., 2014). They are also powerful tools to study digestion when considering ethical, practical, and economic factors. Minekus et al. (2014) built a standardised static *in vitro* digestion model that has been used widely in different food studies (Lin et al., 2020; Bustos, Vignola, Pérez, & León, 2017; Di Nunzio et al., 2020).

Different techniques have been used to determine the products of food after digestion. For instance, the peptides released by *in vitro* digestion of meat were identified and characterised using liquid crystal-electrospray ionization tandem mass spectroscopy (Escudero et al., 2010), and high performance liquid chromatography and matrix-assisted laser desorption/ionisation time-of-flight mass spectrometry (Ferranti et al., 2014). However, most studies of baked food have focused on predicting the glycaemic index by measuring the *in vitro* digestive stability of certain compounds, such as starch and protein (Assad-Bustillos et al., 2020; Eslava-Zomeño et al., 2016; Noor Aziah et al., 2011; Quiles et al., 2018). There have been no studies focusing on

metabolite release of sponge cake after digestion, as well as the effect of dietary fibre on the metabolite release of sponge cake.

Proton nuclear magnetic resonance (^{1}H NMR) has been used widely to identify metabolites. This technique analyses the sample as a whole and no preliminary separation among compounds is required. The key information provided by this technique is associated with the signals' position and their corresponding area in the spectrum, as well as the multiplicity or splitting of signals HSQC [1]H–[13]C correlation table and/or [1]H–[13]C 2D spectra (Lou, Zhai, & Yang, 2021; Vidal et al., 2016; Zhao, Zhao, Wu, Lou, & Yang, 2019; Zhao, Chen, Wu, He, & Yang, 2020).

Furthermore, the overall breakdown of a meal during digestion can be described via its rheological properties. Rheological properties (deformation and flow) of food products have great influence on the transportation, hydrolysis and absorption of hydrolysed nutrients within the gastrointestinal tract (Abu-Jdayil, 2003; Keppler et al., 2020; Wu et al., 2016). For instance, it was reported that the increased viscosity of the digesta can decline the rate of gastric evacuation, which correlates positively with lowering the glycaemic response and extend satiety with food intake (Hoad et al., 2004; Kristensen and Jensen, 2011; Lentle and Janssen, 2008; Zhu et al., 2013). An increase in intestinal viscosity might lead to lower nutrient mixing and absorption (Bornhorst et al., 2013).

In order to develop healthy food, different dietary fibres are added in many food products. In small intestinal simulation, the addition of

---

* Corresponding author at: Department of Food Science and Technology, National University of Singapore, Singapore 117543, Singapore.
  E-mail address: fstynghs@nus.edu.sg (H. Yang).

soluble dietary fibres exhibit viscous characteristics, which are beneficial for physiological responses related to viscosity, such as blood glucose attenuation (Dikeman et al., 2006; Kristensen and Jensen, 2011). One of the dietary fibres, konjac glucomannan, increased the gel structures of cheese pies during *in vitro* digestion and produced harder and more cohesive pies, which is useful for stimulating higher anticipatory satiation capacity due to the increase of time and effort in mouth handling at the time of consumption (Marcano et al., 2015). However, knowledge of the rheological behaviour of more variety of food with dietary fibres after digestion is still in its infancy.

Sponge cake is one of the most widely consumed baked goods. Recently, dietary fibre from different sources have been applied to replace wheat flour partially or totally to develop high dietary fibre content sponge cakes (Lu et al., 2010; Sudha et al., 2007), including *Eucheuma*, which is a kind of red seaweed containing about 69.33% dietary fibre (Huang, Theng, Yang, & Yang, 2021; Huang and Yang, 2019). Yang and Yang (2020) proved that the polysaccharides extracted from *Eucheuma* mainly comprises carrageenan (Huang, Zhao, & Yang, 2021). Furthermore, the carrageenan oligosaccharide extracted from *Eucheuma* and prepared by enzymatic degradation has benefits for health such as antioxidation capability (Mou, Jiang, & Guan, 2003; Xu et al., 2017).

This study aimed to evaluate the effect of *Eucheuma* on the evolution of cake nutrients after *in vitro* digestion, and to better understand the rheological characteristics of sponge cake after *in vitro* digestion. ^{1}H NMR analysis of metabolites, glucose release measurements, rheological tests (including steady shear flow and frequency sweep tests), and microstructure tests were conducted. This study lays the foundation for the future optimisation of food properties to control their digestive characteristics and better understand the effect of dietary fibre on metabolites of food.

2. Materials and methods

2.1. Materials

Cake flour (11.9% moisture, 8.1% protein) was pruchased from PRIMA RND (Prima Group, Singapore, Singapore); the cake emulsifier (composes of emulsifier, sorbitol, propylene glycol, potassium hydroxide, and permitted colouring) was provided by Liang San Food Industry Company (Pantech Industrial Complex, Singapore, Singapore); the canola oil was obtained from Lam Soon (Lam Soon Singapore PTE LTD, Singapore, Singapore). To simulate *in vitro* digestion, α-amylase (EC 3. 2. 1. 1, from porcine pancreas, 10 U/mg), pepsin (EC 3. 4. 23. 1, from porcine gastric mucosa, 4177 U/mg), pancreatin (EC 232. 468. 9, from porcine pancreas, contains amylase, trypsin, lipase, ribonuclease, and protease; 96.7 U/mL based on trypsin activity), and bile were obtained from Sigma-Aldrich Chemie GmbH (Steinheim, Germany). All the other chemicals were of analytical grade and were also purchased from Sigma-Aldrich Chemie GmbH.

2.2. Preparation of sponge cakes

In our previous study, *Eucheuma* was used as a flour replacer to make high dietary fibre sponge cakes. The replacement percentages were 5%, 10%, 15% and 20%, respectively (Huang and Yang, 2019). In the present study, the EP20 sample (20% replacement of cake flour with *Eucheuma*) was chosen as a representative sample because of its highest replacer content. As described in our previous study (Huang and Yang, 2019), first 200 g of whole eggs, 100 g of sugar, and 8 g of cake emulsifier were mixed in the mixer (KitchenAid, St Joseph, MI, USA) for 8 min at speed 6, then 100 g of the sifted flour (or *Eucheuma* powder and flour) and 25 g of canola oil were added and mixed for 2 min at speed 1 separately. The cake batter (250 g) was transferred into a 6$^#$ baking tin (external diameter of 160 mm, height of 57 mm) and baked in a convection oven (Fabricant Eurfours®, Gommegnies, France,) at 180 °C for 30 min to make the sponge cake.

2.3. In vitro digestion of sponge cakes

A three-stage *in vitro* digestion model simulating oral, gastric, and intestinal conditions, as described by Minekus et al. (2014), was applied in this study with some modifications. The electrolyte stock solutions, including simulated salivary fluid (SSF), simulated gastric fluid (SGF), and simulated intestinal fluid (SIF), were prepared as shown in Table A1. The total protein content of all the samples was measured using kjeldahl determination before digestion by FOSS Kjeltec System AN300 (FOSS, Denmark). In the oral phase, 4 mL of α-amylase solution (final enzyme activity = 75 U/mL) prepared using SSF, 25 μL of 0.3 mol/L CaCl₂, and 0.975 mL of distilled water were added to produce a final volume of 5 mL. Then, 15 μL of 1 mol/L HCl was added to adjust the pH and the mixture was warmed to 37 °C in a water bath. The minced sponge cake samples (5 g) were added into the mixed solution and incubated at 37 °C for 2 min with shaking (200 rpm).

To perform the simulated gastric digestion, 8 mL of pepsin solution (final enzyme activity = 2000 U/mL) prepared using SGF, 5 μL of 0.3 mol/L CaCl₂, 0.65 mL of 1 mol/L HCl, and 1.345 mL of distilled water were added and warmed at 37 °C. Afterwards, the total liquid mixture was added into the oral phase products. The final pH values were 3.0 and the final mixture was incubated at 37 °C for 2 h with shaking (200 rpm).

To simulate intestinal digestion, 16 mL of pancreatin solution (final enzyme activity = 100 U/mL based on trypsin activity), 40 μL of 0.3 mol/L CaCl₂, 0.1768 g of bile, 400 μL of 1 mol/L NaOH, 3.48 mL distilled water, and 80 μL of amyloglucosidase were mixed and warmed up at 37 °C. Afterwards, the total liquid mixture was added into gastric phase products. The final pH value was 7.0 and the final mixture was incubated at 37 °C for 2 h with shaking (200 rpm). After simulated intestinal digestion, samples were transferred into boiling water to stop the enzyme activity and then used for further analysis.

2.4. NMR analysis

The trichloroacetic acid (TCA) extraction was carried out first. The minced sponge cake samples were separately mixed with a 7.5% TCA aqueous solution at a ratio of 1:2 (w:v). Then, the mixture was filtered using filter paper (Whatman No.4, Buckinghamshire, UK) and centrifuged (12000g, 10 min) to remove the precipitates. The supernatants (SF) were filtered through a microporous membrane (0.22 μm), 1 mL was transferred into centrifuge tubes, and then the samples were freeze-dried for further analysis. For the cake samples after *in vitro* digestion, the supernatant containing metabolites was centrifuged at 5000g for 5 min. The supernatants were filtered through a microporous membrane (0.22 μm), 1 mL was transferred into centrifuge tubes for freeze-drying. The α–amylase, pepsin, pancreatin, and bile were dissolved in water separately with final concentrations that were the same as those in the intestinal phase, to evaluate their spectral signals in the spectra of the samples collected during digestion.

The freeze-dried sample was dissolved in deuterated water (D₂O, 99.9%) containing 0.005% sodium 3-trimethylsilyl [2,2,3,3-d₄] propionate (TSP) and centrifuged (12000g, 10 min, 4 °C). Then, 600 μL of the supernatants were pipetted into NMR tubes with 5 mm diameter. A NMR spectrometer (DRX-500, Bruker, Rheinstetten, Germany) with a frequency of 500.23 MHz was applied. The standard NOESY setting (noesypr1d) was performed to record the ^{1}H spectrum with a width of 10.0 ppm (Zhao et al., 2020). The 1D spectra were got by 128 scans and an automatic pulse calculation experiment (pulsecal) was performed to modify the 90° pulse length. For the subsequent identification of metabolic chemicals, the 2D ^{1}H–^{13}C heteronuclear single quantum coherence spectroscopy (HSQC) of the samples was gained using the Bruker hsqcedetgpsisp2.3 pulse sequence at 25 °C. The ^{1}H spectra (width of 10.0 ppm) and the ^{13}C spectra (width of 180.0 ppm) were acquired in the F2 and F1 channels, respectively.

2.5. Spectra processing and analysis

The baseline and phase distortions of the 1D ^{1}H spectra were manually corrected using the TopSpin 3.6.0 (Bruker) software. The 1D ^{1}H and 2D ^{1}H–^{13}C spectra helped to conduct the metabolic identification cooperatively. The chemical shifts were checked and verified by the Human Metabolome Database (http://www.hmdb.ca/), the Biological Magnetic Resonance Data Bank (http://www.bmrb.wisc. edu/metabolomics), the Madison Metabolomics Consortium Database (http://mmcd.nmrfam.wisc.edu), and related references (Chen et al., 2020; Vidal et al., 2016). The ^{1}H signal peaks (0.0–10.0 ppm) were integrated and normalised to the TSP peak area at 0.0 ppm. The deuterium oxide region between 4.80 and 5.00 ppm was excluded from the analysis as it contains residual water resonance. The region buckets (0.01 ppm width) were split from the normalised spectra and the collected binned data were used for analysis. The obtained NMR data were evaluated by principal component analysis (PCA) and orthogonal projection to latent structures-discriminant analysis (OPLS–DA) using SIMCA software (version 13.0, Umetrics, Umeå, Sweden). Moreover, variable importance in projection (VIP) analysis was performed.

2.6. Released glucose measurement and mathematical modelling

During intestinal digestion, samples were taken at different times (0, 5, 10, 15, 30, 45, 60, 75, 90, and 120 min), transferred into centrifuge tubes, and immediately heated in boiling water to stop the enzymatic reaction. Then, the digesta were centrifuged at 12000g for 15 min. The supernatants were analysed using a Glucose (GO) Assay Kit (GAGO20, Sigma) following the manufacturer's instructions. The released glucose concentration was calculated as follow:

$$C_t = M_t - M_0 \tag{1}$$

where C_t means the concentration of released glucose (mg/mL) at time t, M_t means the total concentration of glucose (mg/mL) at time t, and M_0 means the concentration of glucose (mg/mL) at time 0 in the supernatants.

To evaluate the digestive profile of different sponge cake samples, the starch digestion curves were modelled based on following Eq. (2) (Goñi, Garcia-Alonso, & Saura-Calixto, 1997).

$$C_t = C_\infty \left(1 - e^{-kt}\right) \tag{2}$$

where C_∞ means the equilibrium concentration of glucose (mg/mL), k means the rate constant of starch digestion (min^{-1}), and t represents time (min). Linear-least-squares regression of Eq. (2) was performed to calculate the corresponding values of C_∞ and k through minimizing the root mean square error (RMSE) using Matlab software (R2014b, the MathWorks Inc., Natick, MA, USA). The RMSE and R^2 were used to determine the quality of the established model.

2.7. Rheological tests

Rheological measurements were performed by a MCR 102 stress-controlled rheometer (Anton Paar, Graz, Austria). The samples were relaxed at 37 °C for 5 min and covered with a thin layer of oil to avoid evaporation (Yang et al., 2020; Takahashi, Kurose, Okazaki, & Osako, 2016). The measurements were performed at 37 °C with a fixed gap of 1 mm (25 mm plate-plate geometry). Each sample was measured in triplicate, prepared on different days by *in vitro* digestion. The referent hydrated samples were made by adding the same amount of water containing no enzymes for each sponge cake and adjusting them to the same pH used during digestion. The strain sweep measurement was performed in a range of 0.01–100% and with an angular frequency of 1 Hz to determine the linear viscoelastic region (LVR) of all samples. The steady shear flow test was performed over a shear rate of 0.01–10 s^{-1}. The frequency sweep test was performed over frequencies of 0.1 to 100
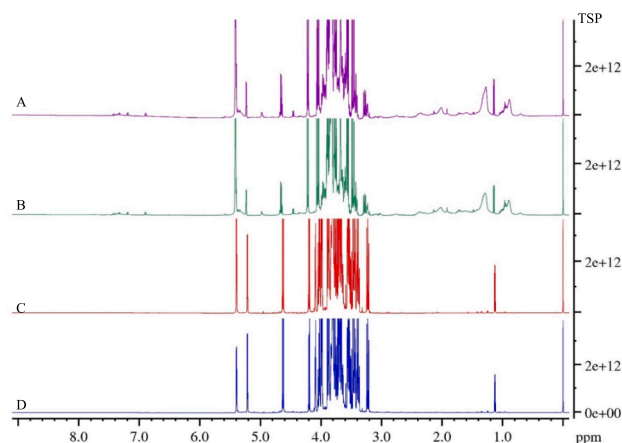

Fig. 1. ^{1}H nuclear magnetic resonance (NMR) spectra of sponge cake samples after *in vitro* digestion. (A)–(D) represent the control cake after *in vitro* digestion, an EP20 cake after *in vitro* digestion, the SF sample of the control cake, and the SF sample of the EP20 cake, respectively. EP20 means cakes prepared with 20% replacement of cake flour using *Eucheuma* powder. SF sample means the sample made by extracting the minced cake samples with trichloroacetic acid (TCA) before digestion.

rad/s at a strain amplitude of 0.1% (within the LVR).

2.8. Microstructure test

The surface structure of the digesta after digestion was showed using scanning electron microscopy (SEM) (Phenom ProX, Phenom-World BV, Eindhoven, Netherlands). The freeze-dried samples were sprayed on an aluminium plate using double-sided adhesive and coated with a thin film of gold. The samples were examined at an accelerating voltage of 10 kV. Each image was taken at a magnification of 2000×.

2.9. Statistical analysis

Each quantitative value represents the mean of triplicate measurements, with the associated standard deviation. Differences between treatments were analysed using the one-way analysis of variance, as conducted in the statistical software MS office Excel 2020 (Microsoft, Redmond, WA, USA). Differences with a P value < 0.05 were considered statistically different.

3. Results and discussion

3.1. Metabolites identification and comparison

The metabolic ^{1}H spectra of the control cake and EP20 cake after *in vitro* digestion are shown in Fig. 1A and B. The two spectra presented similar overall chemical shifts, indicating similar chemical profiles of cake samples after *in vitro* digestion. The main ^{1}H peaks were in the range of 0.5–5.5 ppm. This region typically includes metabolites such as free amino acids, aliphatic acids, and saccharides (Chen et al., 2020). These results identify with some previous research that sponge cake is rich in carbohydrates, proteins, and lipids (Assad-Bustillos et al., 2020; Wilderjans et al., 2013). The qualitative identification of metabolic peaks was performed and summarised in Table 1 based on the 2D spectrum and 1D binned area datasets.

Overall, 22 compounds including saccharides, amino acids, fatty acids, and other metabolites were identified (Fig. 2, Table 1). The ^{1}H signals in the region around 0.8–3.0 ppm represented amino acids (e.g. isoleucine, leucine) and fatty acids (e.g. linoleic acid, palmitic acid). Soluble saccharides, including α-D-glucose, β-D-glucose, sucrose, maltose, and fructose were identified in the region around 3.0–5.5 ppm.

Table 1

Assignment of certain signals of the ^{1}H NMR spectra of sponge cake samples after *in vitro* digestion, together with their chemical shifts and multiplicities.

	Metabolites	Assignments	[1]H chemical shifts (ppm) and multiplicity [a]
1	Linoleic acid	C_9H,$C_{10}H$, $C_{12}H$,$C_{13}H$; $C_{11}H_2$; C_2H_2; C_8H_2, $C_{14}H_2$; C_3H_2;C_4H_2-C_7H_2, $C_{15}H_2$-$C_{17}H_2$; $C_{18}H_3$	5.37 (m); 2.76 (t); 2.36 (t); 2.01 (m); 1.65 (m); 1.28 (m); 0.89 (t)
2	Oleic acid	$C_{11}H_2$; C_3H_2; C_8H_2, $C_{11}H_2$; C_9H,$C_{10}H$; C_4H_2-C_7H_2, $C_{12}H_2$-$C_{16}H_2$; $C_{18}H_3$	2.36 (t); 1.65 (m); 2.01 (m); 5.34 (m); 1.28 (m); 0.89 (t)
3	Palmitic acid	C_2H_2; C_3H_2; C_4H_2-$C_{15}H_2$; $C_{16}H_3$	2.36 (t); 1.65 (m); 1.28 (m); 0.89 (t);
4	Isoleucine	αCH; βCH; γCH$_2$; γ'CH$_3$; δCH$_3$	3.67 (d); 1.95 (m); 1.46 (m), 0.96 (d); 0.93 (t)
5	Leucine	αCH; βCH$_2$, γCH; δCH$_3$, δ'CH$_3$	3.72 (m); 1.70 (m); 0.96 (t)
6	Valine	αCH; βCH; γCH$_3$; γ'CH$_3$	3.60 (d); 2.25 (m); 0.98 (d); 1.04 (d)
7	Alanine	αCH; βCH$_3$	3.78 (q); 1.48 (d)
8	Proline	CH; βCH$_2$; γCH$_2$	4.12 (dd); 2.33, 2.12 (m); 2.02 (m)
9	Glutamine	αCH; βCH$_2$; γCH$_2$	3.77 (m); 2.15 (m); 2.44 (m)
10	Aspartic acid	αCH; βCH$_2$	3.81 (m); 2.67, 2.82 (m)
11	Asparagine	αCH; βCH$_2$	3.99 (q); 2.88 (dd)
12	Choline	-N-(CH$_3$)$_3$; -N-CH$_2$; -O-CH$_2$	3.21 (s); 3.52 (m); 4.01 (m)
13	Glycine	CH$_2$	3.55 (s)
14	Maltose	^{1}C$_1$H; ^{1}C$_2$H; ^{1}C$_3$H; ^{1}C$_4$H; ^{1}C$_5$H; ^{1}C$_6$H$_2$; ^{2}C$_1$H; ^{2}C$_2$H; ^{2}C$_3$H; ^{2}C$_4$H; $^{2\alpha\beta}$C$_5$H; ^{2}C$_6$H$_2$	5.24 (d); 3.70 (m); 3.54 (t); 3.42 (t); 3.68 (m); 3.76 (m); 5.42 (dd); 3.33 (t); 3.91 (m); 3.70 (m); 3.67, 3.83 (m); 3.82 (m)
15	Serine	αCH; βCH$_2$	3.83 (t); 3.94 (m)
16	Fructose	C$_1$H$_2$; C$_2$H; C$_3$H; C$_4$H; C$_6$H$_2$	3.63 (m); 3.93 (m); 3.87 (m); 3.89 (d); 3.71 (d)
17	β-D-Glucose	C$_1$H$_2$; C$_2$H; C$_3$H; C$_4$H; C$_5$H; C$_6$H	3.70 (m); 3.52 (m); 3.46 (m); 3.39 (m); 3.24 (dd); 4.45 (d)
18	α-D-Glucose	C$_1$H$_2$; C$_2$H; C$_3$H; C$_4$H; C$_5$H; C$_6$H	3.78 (m); 3.82 (m); 3.49 (m); 3.71 (m); 3.70 (m); 5.24 (d)
19	Sucrose	^{1}C$_1$H; ^{1}C$_2$H; ^{1}C$_3$H; ^{1}C$_4$H; ^{1}C$_5$H; ^{1}C$_6$H$_2$; ^{2}C$_1$H$_2$; ^{2}C$_2$H; ^{2}C$_3$H; ^{2}C$_4$H; ^{2}C$_5$H; ^{2}C$_6$H$_2$	5.42 (d); 3.47 (t); 3.55 (dd); 3.42, 3.51 (t); 3.84 (m); 3.59 (dd); 3.59 (dd); 3.93 (m); 4.05 (m); 4.21 (d); 3.57 (dd)
20	Tyrosine	C$_1$H; C$_2$H$_2$; C$_4$H; C$_5$H	3.90 (dd); 3.01, 3.17 (dd); 7.19 (d); 6.90 (m)
21	Phenylalanine	C$_1$H; C$_2$H$_2$; C$_4$H; C$_5$H; C$_6$H	3.97 (m); 3.27 (m); 7.31 (m); 7.41 (m); 7.36 (m)
22	Tryptophan	C$_1$H; C$_2$H$_2$; NC$_4$H; C$_6$H; C$_7$H; C$_8$H; C$_9$H	4.01 (dd); 3.46, 3.29 (dd); 7.71 (d); 7.53 (d); 7.31 (s); 7.23 (m); 7.20 (m)

[a] Multiplicity: s, singlet; d, doublet; t, triplet; q, quartet; dd, doublet of doublets; m, multiplet.

Lastly, the ^{1}H peaks in the region of 6.5–8.0 ppm also suggested the existence of amino acids such as tryptophan, phenylalanine, and tyrosine. The results were in accordance with the components of sponge cake (Assad-Bustillos et al., 2020; Wilderjans et al., 2013) and the metabolites of food after *in vitro* digestion, such as fish (Vidal et al., 2016) and cheese (Bordoni et al., 2011).

The ^{1}H spectra of the SF acquired from the control cake sample and the EP20 sample are shown in Fig. 1C and D. The results showed that the SF samples of the control and EP20 cakes had the same features and were very similar. The signals were mainly generated by saccharides, such as sucrose, maltose, α-D-glucose, and fructose. These hydrophilic compounds are present in cakes because the main recipe of sponge cake includes a high amount of sugar and flour (Slade, Kweon, & Levine, 2020).

The unsupervised PCA was conducted to provide an overview of samples similarities and dissimilarities, clustering and deviating features. The model quality parameters were $R^2X = 0.954$ and $Q^2 = 0.926$ (Fig. 3A), suggesting that the model had good explanatory and predictive ability. The PCA score plot (Fig. 3B) showed, along the PC2, a good clustering of the samples from the same group. The SF samples did not separate clearly from each other; however, the samples after *in vitro* digestion had distinct separations, indicating distinct metabolic changes in the control cake sample and EP20 sample after *in vitro* digestion. The loading plot can provide information about the metabolites that mostly contributed to the separation of sample groups. Fig. 3C showed that most of the metabolites, e.g. tyrosine, linoleic acid, β-D-glucose, and aspartic acid, had large loading on PC2, while PC1 was characterised by several metabolites such as glycine, choline, and isoleucine. These metabolites might represent marker metabolites that responded to the addition of *Eucheuma* in the sponge cake recipe.

The supervised OPLS-DA was applied to detect the discriminant metabolites between the control group and EP20 group samples after digestion. There was no significant difference in total protein content between control and EP20 cakes before digestion (data not shown). The established OPLS-DA models showed good predictive and explanatory ability according to the R^2 and Q^2 values (0.997 and 0.991, respectively). Furthermore, the score plot of the OPLS–DA model (Fig. 3D) demonstrated clear separation between the control group and the EP20 group. The results indicated that the addition of *Eucheuma* to the sponge cake recipe had a detectable effect on metabolite release. Coefficient plots (Fig. 3E) were applied statistically to identify significant metabolites in paired groups after digestion. The results revealed that 14 metabolites (e.g. valine, glutamine, linoleic acid) showed decreased relative contents in the EP20 sample after *in vitro* digestion compared with those in the control sample. The metabolites (β-D-glucose, aspartic acid, and asparagine) with a VIP value > 1 were recognised as significant compounds (Fig. 3E). Many previous studies claimed that the
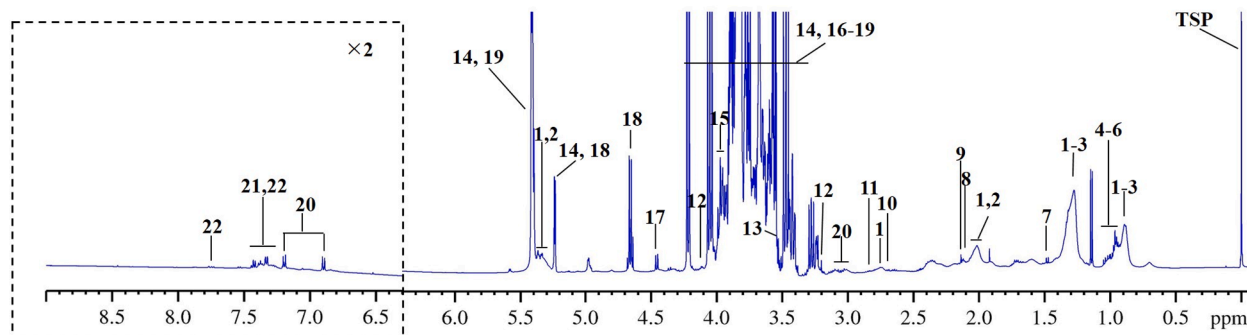

Fig. 2. Metabolic identification of a representative sponge cake after *in vitro* digestion. Note: 1, Linoleic acid; 2, Oleic acid; 3, Palmitic acid; 4, Ile; 5, Leu; 6, Val; 7, Ala; 8, Pro; 9, Gln; 10, Asp; 11, Asn; 12, Choline; 13, Gly; 14, Maltose; 15, Ser; 16, Fructose; 17, β-D-Glucose; 18, α-D-Glucose; 19, Sucrose; 20, Tyr; 21, Phe; 22, Trp.
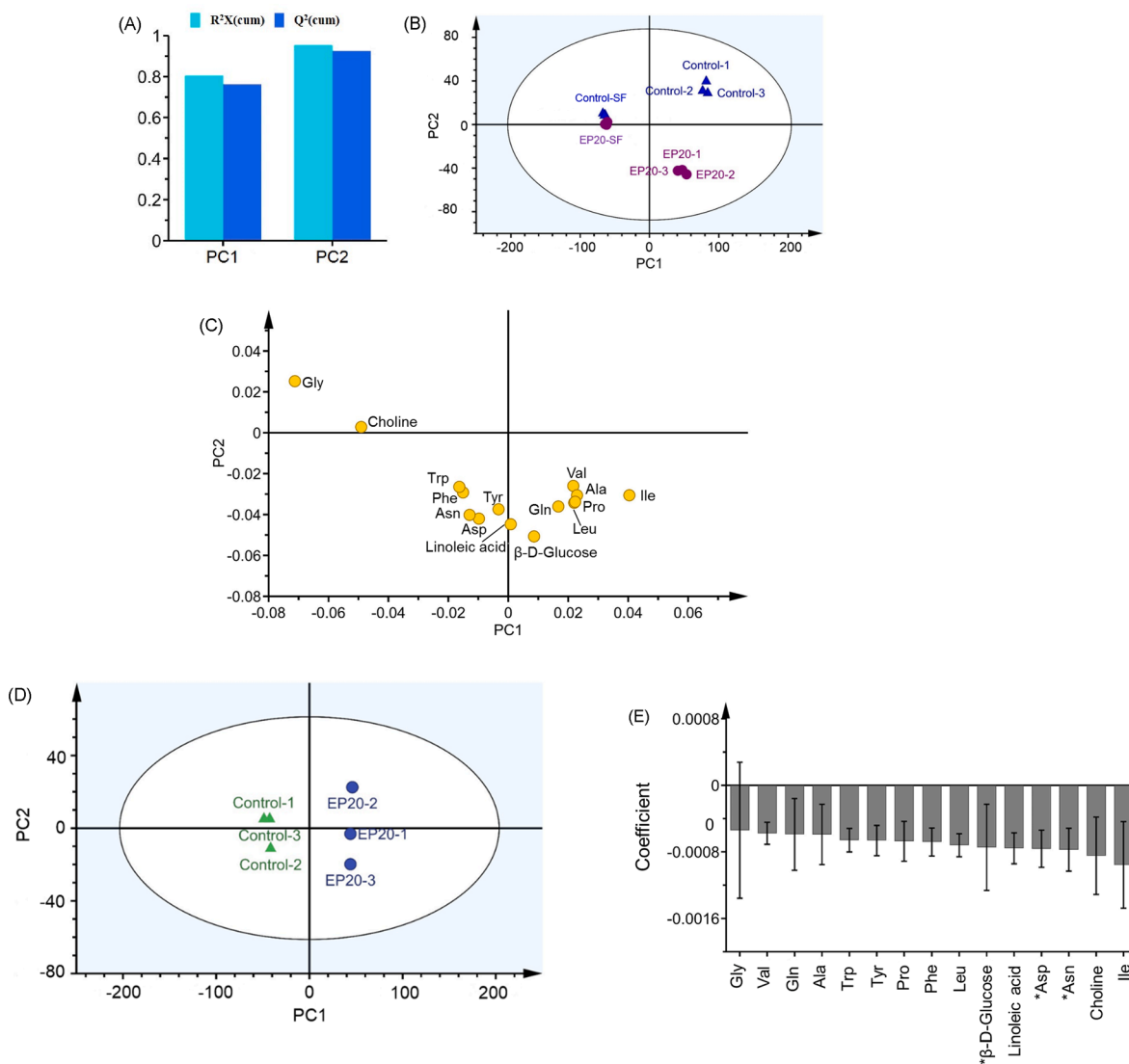
Fig. 3. (A) The principal components explaining variances used in principal components analysis (PCA); (B) PCA score plot; (C) PCA loading plot; (D) Orthogonal projection to latent structures-discriminant analysis (OPLS-DA) score plot of a control cake and an EP20 cake after *in vitro* digestion. (E) OPLS-DA coefficient plot of a control cake and an EP20 cake after *in vitro* digestion; the metabolite marked with * has a variable importance in projection (VIP) value > 1, indicating a significant contribution to the OPLS-DA models. EP20 means cakes prepared with 20% replacement of cake flour using *Eucheuma* powder. SF sample means the sample made by extracting the minced cake samples with trichloroacetic acid (TCA) before digestion.

addition of dietary fibres reduced the protein and fat digestibility after digestion resulting from the possible complex formation between the fibre components and the protein or fat fraction (Bilgiçli et al., 2007; Dégen et al., 2007; Opazo-Navarrete et al., 2019). This was also demonstrated in the present study by the reduced amino acid contents (valine, glutamine, and alanine) and fatty acid contents (linoleic acid) in the EP20 sample compared with those in the control sample.

3.2. Glucose release and mathematical modelling

NMR performs poorly when analysing saccharides because they cannot be separated clearly on the spectra. Thus, the released glucose during intestinal digestion was measured as representative data. Fig. 4A shows the release of glucose during intestinal digestion of different cake samples. The released glucose concentration of the control sample was always higher than that of the EP20 sample. At the end of intestinal digestion, the glucose concentration of the EP20 sample was reduced by 37.3%. The hollow circle in Fig. 4A represents the theoretical values of EP20 containing 100% flour, and this theoretical value at 120 min was

significantly lower than that of the control sample. Thus, *Eucheuma* replacement decreased the glucose release during *in vitro* digestion. This could be caused by the ability of dietary fibre to suppress glucose diffusion. Previous studies showed that a variety of viscous fibres in meals reduced glucose release under both *in vivo* and *in vitro* conditions (Brennan et al., 2012; Chawla and Patil, 2010; Fabek et al., 2014; Foschia et al., 2015). Fabek et al. (2014) highlighted the relationship between fibre viscosity and glucose diffusion during digestion and found that all gums are able to reduce the glucose response curve. In the present study, *Eucheuma* contained a high amount of dietary fibre, which could also slow starch digestion and reduce the amount of diffused glucose.

To describe the glucose release results quantitatively, mathematical modelling was developed for all samples. The values of the digestion rate constant k and the equilibrium concentration C_∞ in Eq. (2) are summarised in Table 2. Notably, the C_∞ value of the EP20 sample changed significantly comparing with that of the control sample in the intestinal phase; however, the k value of EP20 was not significantly different to that of the control sample. The equilibrium glucose concentration was
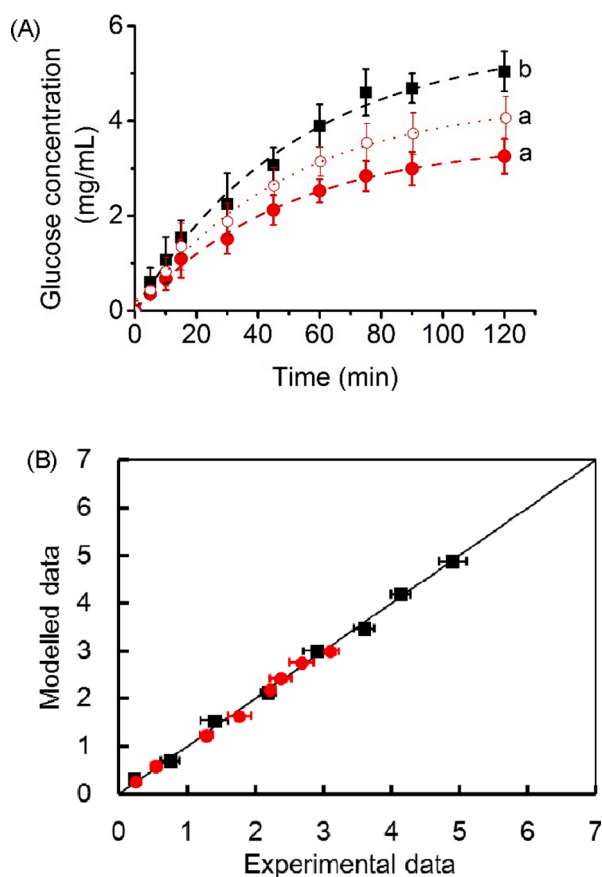
Fig. 4. (A) The glucose concentration during digestion and the corresponding developed mathematical models (dashed line) after *in vitro* digestion. The different letters indicate that the values were significantly different ($P < 0.05$). (B) The validation plots for the modelled data against the experimental data. ■, Control cake; ●, EP20; ○, the theoretical values of EP20 containing 100% flour. EP20 means cakes prepared with 20% replacement of cake flour using *Eucheuma* powder.

Fig. 5. (A) The viscosity of samples after *in vitro* digestion. ■, Hydrated control cake; □, control cake after digestion; ▲, hydrated EP20 sample; △, EP20 after digestion. (B) Comparison of storage modulus (G') and loss modulus (G'') of samples after *in vitro* digestion. ■/□, Hydrated control cake; ●/○, control cake after digestion; ◆/◇, hydrated EP20 sample; ▲/△, EP20 after digestion. EP20 means cakes prepared with 20% replacement of cake flour using *Eucheuma* powder.

Table 2
Mathematical modelling parameters for glucose release during gastric and intestinal digestion.

Samples	k (min^{-1})	C_∞ (mg/mL)	R^2	RMSE
Control cake	0.019 ± 0.002 [A]	5.679 ± 0.241 [A]	0.996	0.161
EP20	0.021 ± 0.001 [A]	3.562 ± 0.095 [B]	0.998	0.072

Values represent the mean with standard deviation. Values with different superscripts in uppercase letters are significantly different across sponge cake types ($P < 0.05$). EP20 means cakes prepared with 20% replacement of cake flour using *Eucheuma* powder.

lower than that of control; however, the starch digestion rate of EP20 was similar to that of the control.

Table 2 also shows the RMSE and R^2 values. All the RMSE values were very small, suggesting that the quality of the established model was appropriate. Furthermore, additional experiments were conducted to validate the models (Fig. 4B). The data points were evenly distributed around the 45° line, suggesting a high accordance between the modelled and experimental results. In addition, the values of R^2 were high, which further confirmed that the model was adequate for the task.

3.3. Viscosity of the different digesta

Fig. 5A shows the dependence of the apparent viscosity on the shear rate of the samples after *in vitro* digestion at 37 °C. The referent samples
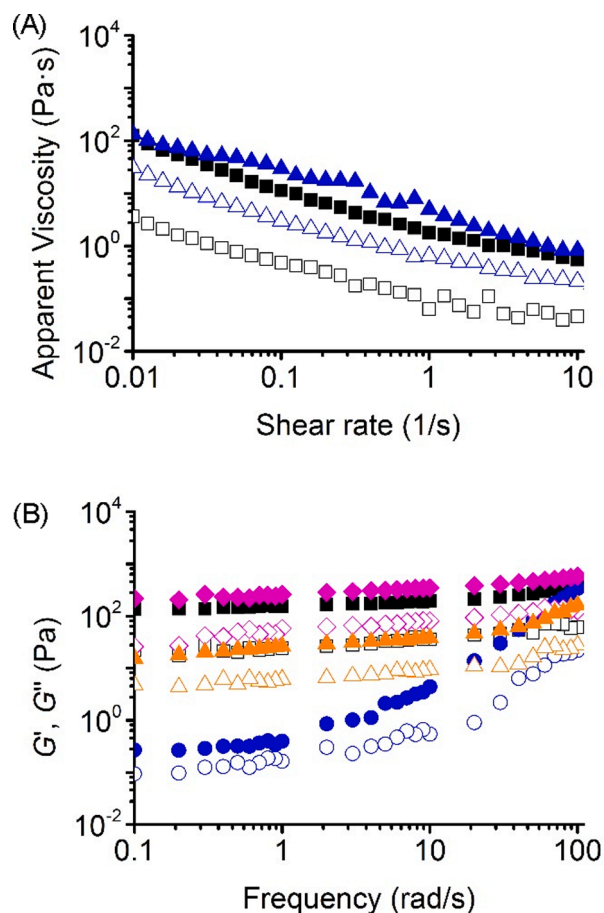
Table 3
Power law parameters for the digesta after oral, gastric, and intestinal digestion.

Samples	Control cake		EP20	
	Before digestion	After digestion	Before digestion	After digestion
Power law parameters				
K (Pa s^n)	1.22 ± 0.09 [b, A]	0.07 ± 0.01 [a, A]	6.79 ± 0.67 [b, B]	0.29 ± 0.04 [a, B]
N	0.03 ± 0.02 [a, A]	0.17 ± 0.03 [b, B]	0.38 ± 0.03 [b, B]	0.02 ± 0.01 [a, A]
R^2	0.998	0.994	0.992	0.996
RMSE	0.789	0.052	2.546	0.378
Frequency at 1 rad/s				
G' (Pa)	153.48 ± 20.41 [b, A]	0.40 ± 0.26 [a, A]	260.65 ± 65.71 [b, A]	26.39 ± 0.91 [a, B]
G'' (Pa)	24.40 ± 1.36 [b, A]	0.06 ± 0.03 [a, A]	58.23 ± 26.45 [b, A]	6.18 ± 0.64 [a, B]

Values represent the mean with standard deviation. Values with different superscripts in lowercase alphabets in the same row of the same cake are significantly different after digestion ($P < 0.05$). Values with different superscripts in uppercase alphabets in the same row across sponge cake types are significantly different ($P < 0.05$). EP20 means cakes prepared with 20% replacement of cake flour using *Eucheuma* powder.
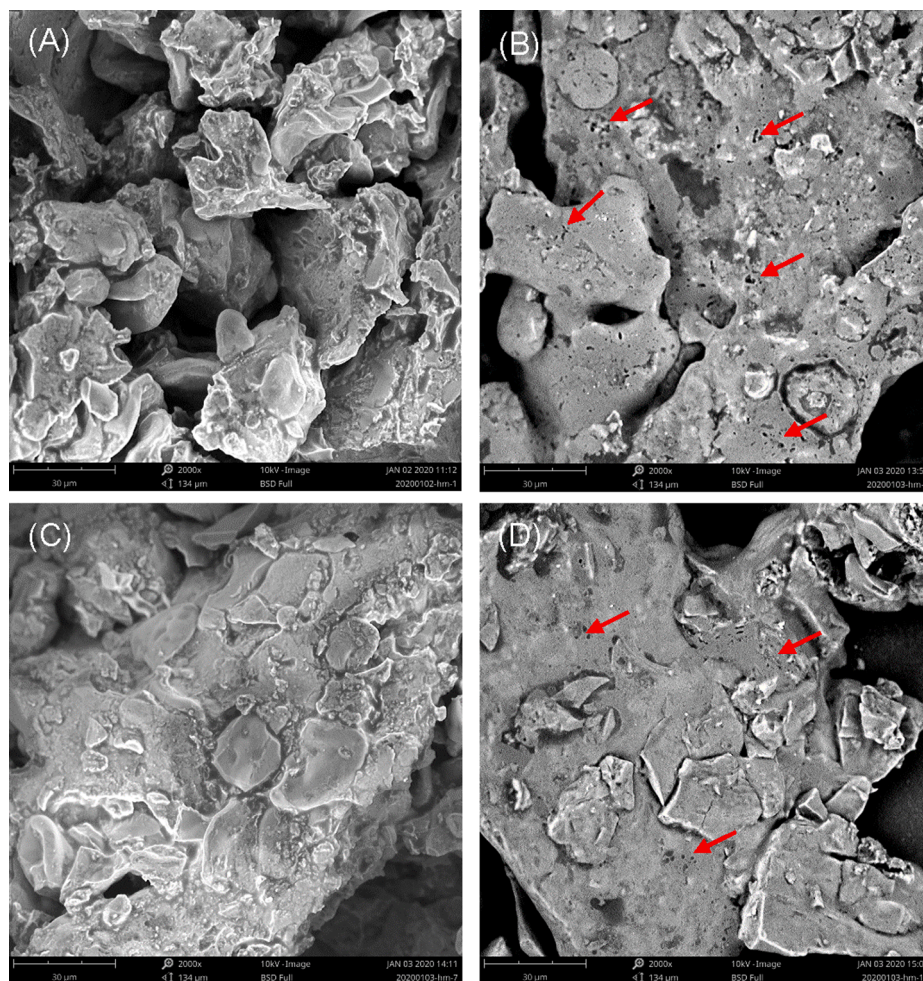
Fig. 6. Micrographs of the control cake and EP20 samples before and after *in vitro* digestion. (A) Hydrated control cake, (B) control cake after digestion, (C) hydrated EP20 sample, (D) EP20 after digestion. EP20 means cakes prepared with 20% replacement of cake flour using *Eucheuma* powder.

were made by adding the same amount of water containing no enzymes for each sponge cake and adjusting them to the same pH. The apparent viscosity decreased as the shear rate increased, indicating all samples showed shear-thinning behaviour. These are consistent with the viscosity of other dense suspensions and *in vitro/vivo* digesta (Lentle and Janssen, 2008; Patarin et al., 2015; Wu et al., 2016). The viscosity of the samples after enzyme digestion was lower than that of the relevant controls at the same shear rate. This was owing to the enzymatic effect, which would lead to the breakdown of cake particles in the suspensions (Wu et al., 2016).

The following power-law equation can be used to describe the data in Fig. 5A:

$$\eta = K \cdot \dot{\gamma}^{n-1} \tag{3}$$

where η represents the apparent viscosity (Pa s), K means consistency coefficient (Pa s^n), $\dot{\gamma}$ means shear rate (s^{-1}), and n represents flow behaviour index.

The related power-law parameters are summarised in Table 3. The values of R^2 were close to 1, and the RMSE values were small, indicating a good fit of the power-law model to the data points (Table 3). The consistency coefficient K provides information about the consistency of the system. The flow behaviour index n indicates the degree of change in viscosity as the shear rate changes. After *in vitro* digestion, both the control cake and the EP20 cake had a lower consistency index. The K values of EP20 before and after digestion were always higher than the corresponding values of the control cake. The n values of the control

cake increased significantly, while those of the EP20 cake decreased after digestion. The lower the value of the flow behaviour index, the greater the viscosity decreases with shear rate. Thus, *Eucheuma*'s effects on *in vitro* sponge cake digestion were mainly reflected in the change of the flow behaviour index. After digestion, the EP20 digesta became more dependent on shear rate. This might have been caused by the high dietary fibre content of *Eucheuma* in the EP20 sample. Similar trends were found in the *in vivo* digesta of pig fed with diets containing mango powder or pectin, which were abundant in dietary fibre (Wu et al., 2016). Increased viscosity of digesta are beneficial to physiological response, such as blood glucose attenuation (Brown et al., 1999; Lentle and Janssen, 2008). Therefore, sponge cake containing *Eucheuma* should be beneficial to the physiological response post food intaking.

3.4. Viscoelasticity of the different digesta

The frequency sweep test can be used to determine the changes in viscoelastic properties of the samples at different observation times (Ortolan et al., 2017). Fig. 5B shows the evolution of the values of storage modulus (G') and loss module (G'') as a function of the frequency of the sponge cake samples after *in vitro* digestion. All samples showed solid-like behaviour because the values of G' were always higher than values of G'' in the frequency range of 0.1–100 rad/s.

The values of G' and G'' at 1 rad/s of all samples are summarised in Table 3. Before digestion, there was no significant difference between the control cake sample and the EP20 sample. After *in vitro* digestion, the G' and G'' values of both samples became smaller because of the
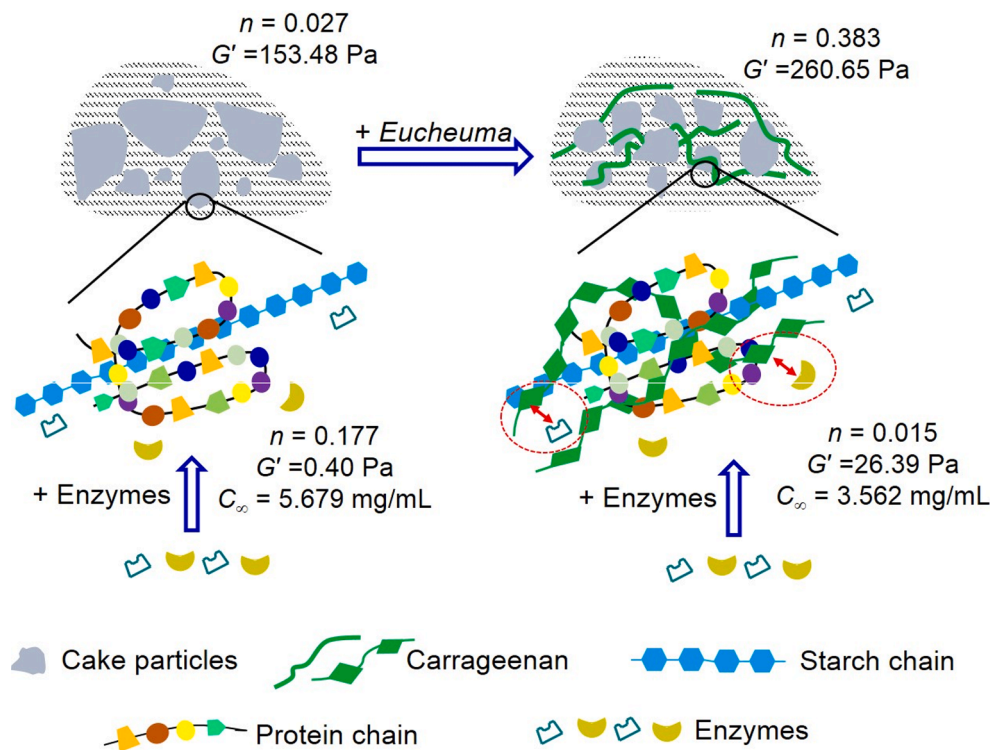
Fig. 7. Schematic model explaining the influence of *Eucheuma* on the *in vitro* digestion of sponge cake.

enzymatic effect and the logical dilution effect of digestive juice. Following oral, gastric, and intestinal digestion, the control cake had the lowest values of both viscoelastic values and became the least structured sample resulting from the major destruction of the cake granules resulted from enzyme action. The EP20 sample had higher values for both viscoelastic moduli than the control sample after digestion, indicating stronger gel behaviour (Fig. 5B). The viscoelastic behaviour of EP20 samples after *in vitro* digestion might be governed mainly by *Eucheuma*. *Eucheuma* contains a high amount of dietary fibre, which mainly comprises of polysaccharides such as carrageenan (Necas and Bartosikova, 2013). Morell, Fiszman, Varela, and Hernando (2014) found that guar gum and λ–carrageenan increased the viscoelastic moduli of milkshakes after *in vitro* oral digestion. Similar trends were also reported by Marcano et al. (2015), who added the konjac glucomannan into cheese pies, contributing to a more structured system after digestion.

3.5. Comparison of microstructure before and after digestion

The SEM images of sponge cake samples obtained after *in vitro* simulation are shown in Fig. 6. Initially, irregular structures formed by starch with distorted outlines embedded in the gluten matrix could be found in both the control cake and the EP20 samples. Most of the starch granules gelatinised after baking, which was consistent with previously published results (Ashwini et al., 2009). Obviously, many holes were formed by the enzymatic effect after *in vitro* digestion, and the control sample presented many more holes than did the EP20 sample. These holes might have resulted in weaker structures of the digesta. This finding was consistent with that of a previous report (Wu et al., 2016), which stated that the surface of the digested diets had many pores due to the enzymatic action and resulted in the changes of rheological properties and plasma glucose response. Thus, these results were in accordance with the rheological results and the reduced sugar release after digestion.

3.6. Schematic model

Based on the results in previous sections, a schematic model was proposed to explain the influence of *Eucheuma* on the *in vitro* digestion of sponge cake (Fig. 7). The addition of *Eucheuma* increased the density of the sponge cake (Huang and Yang, 2019) and produced higher *K*, *n*, *G′*, and *G″* values (Table 3, Fig. 5), indicating that *Eucheuma* could help increase satiety after eating and decreased glucose release during digestion. The main component of *Eucheuma* is carrageenan (Yang and Yang, 2020), which is a type of dietary fibre. Carrageenan may be adhering to some cake components and then prevent the enzymes from reacting with the substrates, resulting in reduced release of amino acids and glucose (Figs. 3 and 4). The reduced numbers of holes in the SEM images of the EP20 sample supported this hypothesis (Fig. 6).

4. Conclusions

The aims of this study were to better understand the metabolite release and the rheological characteristics of sponge cake after *in vitro* digestion and the influence of dietary fibre-enriched flour replacer, such as *Eucheuma*. Overall, 22 compounds, including saccharides, fatty acids, amino acids, and other metabolites, were revealed from NMR spectra. The PCA and OPLS-DA results showed that the *Eucheuma* addition reduced the release of metabolites such as amino acids and fatty acids. The release of glucose from the EP20 sample was reduced by 37.3% in the intestinal phases compared with that of the control cake. A developed mathematical model was used to describe the glucose release results quantitatively. The results of steady shear flow showed that the consistency index decreased for both the control cake and the EP20 cake. *Eucheuma* effects on *in vitro* sponge cake digestion were mainly reflected in the change of the flow behaviour index. All samples showed solid-like behaviour and both viscoelastic moduli decreased after digestion. The results of micrographs showed the formation of many pores on sample surface after digestion and helped explain the rheological results and the reduced release of sugar. The results of the present study could be used as the basis for the future optimisation of food

properties to control their digestive characteristics.

CRediT authorship contribution statement

Min Huang: Conceptualization, Methodology, Investigation, Software, Visualization, Writing - original draft, Writing - review & editing. **Xue Zhao:** Methodology, Software, Visualization. **Yihan Mao:** Methodology, Investigation. **Lin Chen:** Software, Writing - review & editing. **Hongshun Yang:** Conceptualization, Funding acquisition, Project administration, Supervision, Writing - review & editing.

Declaration of competing interest

None.

Acknowledgements

Appendix A. Supplementary material

Supplementary data to this article can be found online at https://doi.org/10.1016/j.foodres.2021.110355.

References

Abu-Jdayil, B. (2003). Modelling the time-dependent rheological behavior of semisolid foodstuffs. *Journal of Food Engineering, 57*(1), 97–102.

Ashwini, A., Jyotsna, R., & Indrani, D. (2009). Effect of hydrocolloids and emulsifiers on the rheological, microstructural and quality characteristics of eggless cake. *Food Hydrocolloids, 23*(3), 700–707.

Assad-Bustillos, M., Palier, J., Rabesona, H., Choiset, Y., Della Valle, G., & Feron, G. (2020). Role of the bolus degree of structure on the protein digestibility during in vitro digestion of a pea protein-fortified sponge cake chewed by elderly. *Journal of Texture Studies, 51*(1), 134–143.

Bilgiçli, N., İbanoğlu, Ş., & Herken, E. N. (2007). Effect of dietary fibre addition on the selected nutritional properties of cookies. *Journal of Food Engineering, 78*(1), 86–89.

Bordoni, A., Picone, G., Babini, E., Vignali, M., Danesi, F., Valli, V., … Capozzi, F. (2011). NMR comparison of in vitro digestion of Parmigiano Reggiano cheese aged 15 and 30 months. *Magnetic Resonance in Chemistry, 49*, S61–S70.

Bornhorst, G. M., Ferrua, M. J., Rutherfurd, S. M., Heldman, D. R., & Singh, R. P. (2013). Rheological properties and textural attributes of cooked brown and white rice during gastric digestion in vivo. *Food Biophysics, 8*(2), 137–150.

Brennan, M. A., Derbyshire, E. J., Brennan, C. S., & Tiwari, B. K. (2012). Impact of dietary fibre-enriched ready-to-eat extruded snacks on the postprandial glycaemic response of non-diabetic patients. *Molecular Nutrition & Food Research, 56*(5), 834–837.

Brown, L., Rosner, B., Willett, W. W., & Sacks, F. M. (1999). Cholesterol-lowering effects of dietary fiber: A meta-analysis. *The American Journal of Clinical Nutrition, 69*(1), 30–42.

Bustos, M. C., Vignola, M. B., Pérez, G. T., & León, A. E. (2017). In vitro digestion kinetics and bioaccessibility of starch in cereal food products. *Journal of Cereal Science, 77*, 243–250.

Chawla, R., & Patil, G. R. (2010). Soluble dietary fiber. *Comprehensive Reviews in Food Science and Food Safety, 9*(2), 178–196.

Chen, L., Zhao, X., Wu, Ji'en, He, Y., & Yang, H. (2020). Metabolic analysis of salicylic acid-induced chilling tolerance of banana using NMR. *Food Research International, 128*, 108796. https://doi.org/10.1016/j.foodres.2019.108796.

Dégen, L., Halas, V., & Babinszky, L. (2007). Effect of dietary fibre on protein and fat digestibility and its consequences on diet formulation for growing and fattening pigs: A review. *Acta Agriculturae Scandinavica, Section A - Animal Science, 57*(1), 1–9.

Diez-Sánchez, E., Llorca, E., Quiles, A., & Hernando, I. (2018). Using different fibers to replace fat in sponge cakes: In vitro starch digestion and physico-structural studies. *Food Science and Technology International, 24*(6), 533–543.

Di Nunzio, M., Picone, G., Pasini, F., Chiarello, E., Caboni, M. F., Capozzi, F., … Bordoni, A. (2020). Olive oil by-product as functional ingredient in bakery products. Influence of processing and evaluation of biological effects. *Food Research International, 131*, 108940. https://doi.org/10.1016/j.foodres.2019.108940.

Dikeman, C. L., Murphy, M. R., & Fahey, G. C. (2006). Dietary fibers affect viscosity of solutions and simulated human gastric and small intestinal digesta. *The Journal of Nutrition, 136*(4), 913–919.

Escudero, E., Sentandreu, M. Ángel., & Toldrá, F. (2010). Characterization of peptides released by in vitro digestion of pork meat. *Journal of Agricultural and Food Chemistry, 58*(8), 5160–5165.

Eslava-Zomeño, C., Quiles, A., & Hernando, I. (2016). Designing a clean label sponge cake with reduced fat content. *Journal of Food Science, 81*(10), C2352–C2359.

Fabek, H., Messerschmidt, S., Brulport, V., & Goff, H. D. (2014). The effect of in vitro digestive processes on the viscosity of dietary fibres and their influence on glucose diffusion. *Food Hydrocolloids, 35*, 718–726.

Ferranti, P., Nitride, C., Nicolai, M. A., Mamone, G., Picariello, G., Bordoni, A., … Capozzi, F. (2014). In vitro digestion of Bresaola proteins and release of potential bioactive peptides. *Food Research International, 63*, 157–169.

Foschia, M., Peressini, D., Sensidoni, A., Brennan, M. A., & Brennan, C. S. (2015). Synergistic effect of different dietary fibres in pasta on in vitro starch digestion? *Food Chemistry, 172*, 245–250.

Goñi, I., Garcia-Alonso, A., & Saura-Calixto, F. (1997). A starch hydrolysis procedure to estimate glycemic index. *Nutrition Research, 17*(3), 427–437.

Hoad, C. L., Rayment, P., Spiller, R. C., Marciani, L., Alonso, B.d. C., Traynor, C., … Gowland, P. A. (2004). In vivo imaging of intragastric gelation and its effect on satiety in humans. *The Journal of Nutrition, 134*(9), 2293–2300.

Huang, M., & Yang, H. (2019). *Eucheuma* powder as a partial flour replacement and its effect on the properties of sponge cake. *LWT - Food Science and Technology, 110*, 262–268.

Huang, M., Theng, A. H. P., Yang, D., & Yang, H. (2021). Influence of κ-carrageenan on the rheological behaviour of a model cake flour system. *LWT - Food Science and Technology, 136*, Article 110324.

Huang, M., Zhao, L., & Yang, H. (2021). Water loss and status in sponge cake: Impact of *Eucheuma* as a flour replacement. *Journal of Food Science, 86*(3), 915–922. https://doi.org/10.1111/1750-3841.15609.

Keppler, S., O'Meara, S., Bakalis, S., Fryer, P. J., & Bornhorst, G. M. (2020). Characterization of individual particle movement during in vitro gastric digestion in the human gastric simulator (HGS). *Journal of Food Engineering, 264*, 109674. https://doi.org/10.1016/j.jfoodeng.2019.07.021.

Kristensen, M., & Jensen, M. G. (2011). Dietary fibres in the regulation of appetite and food intake. Importance of viscosity. *Appetite, 56*(1), 65–70.

Lentle, R. G., & Janssen, P. W. M. (2008). Physical characteristics of digesta and their influence on flow and mixing in the mammalian intestine: A review. *Journal of Comparative Physiology B, 178*(6), 673–690.

Lin, S., Gao, J., Jin, X., Wang, Y., Dong, Z., Ying, J., & Zhou, W. (2020). Whole-wheat flour particle size influences dough properties, bread structure and in vitro starch digestibility. *Food & Function, 11*(4), 3610–3620.

Lou, X., Zhai, D., & Yang, H. (2021). Changes of metabolite profiles of fish models inoculated with *Shewanella baltica* during spoilage. *Food Control, 123*, 107697. https://doi.org/10.1016/j.foodcont.2020.107697.

Lu, T.-M., Lee, C.-C., Mau, J.-L., & Lin, S.-D. (2010). Quality and antioxidant property of green tea sponge cake. *Food Chemistry, 119*(3), 1090–1095.

Marcano, J., Hernando, I., & Fiszman, S. (2015). In vitro measurements of intragastric rheological properties and their relationships with the potential satiating capacity of cheese pies with konjac glucomannan. *Food Hydrocolloids, 51*, 16–22.

Minekus, M., Alminger, M., Alvito, P., Ballance, S., Bohn, T., Bourlieu, C., … Brodkorb, A. (2014). A standardised static in vitro digestion method suitable for food-An international consensus. *Food & Function, 5*(6), 1113–1124.

Mou, H., Jiang, X., & Guan, H. (2003). A κ-carrageenan derived oligosaccharide prepared by enzymatic degradation containing anti-tumor activity. *Journal of Applied Phycology, 15*(4), 297–303.

Morell, P., Fiszman, S. M., Varela, P., & Hernando, I. (2014). Hydrocolloids for enhancing satiety: Relating oral digestion to rheology, structure and sensory perception. *Food Hydrocolloids, 41*, 343–353.

Necas, J., & Bartosikova, L. (2013). Carrageenan: A review. *Veterinarni Medicina, 58*(No. 4), 187–205.

Noor Aziah, A. A., Lee Min, W., & Bhat, R. (2011). Nutritional and sensory quality evaluation of sponge cake prepared by incorporation of high dietary fiber containing mango (*Mangifera indica var. Chokanan*) pulp and peel flours. *International Journal of Food Sciences and Nutrition, 62*(6), 559–567.

Opazo-Navarrete, M., Tagle Freire, D., Boom, R. M., & Janssen, A. E. M. (2019). The influence of starch and fibre on in vitro protein digestibility of dry fractionated quinoa seed (*riobamba variety*). *Food Biophysics, 14*(1), 49–59.

Ortolan, F., Corrêa, G. P., da Cunha, R. L., & Steel, C. J. (2017). Rheological properties of vital wheat glutens with water or sodium chloride. *LWT-Food Science and Technology, 79*, 647–654.

Patarin, J., Blésès, D., Magnin, A., Guérin, S., & Malbert, C. H. (2015). Rheological characterization of gastric juices from bread with different amylose/amylopectin ratios. *Food Digestion: Research and Current Opinion, 6*(1), 2–9.

Quiles, A., Llorca, E., Schmidt, C., Reißner, A.-M., Struck, S., Rohm, H., & Hernando, I. (2018). Use of berry pomace to replace flour, fat or sugar in cakes. *International Journal of Food Science & Technology, 53*(6), 1579–1587.

Slade, L., Kweon, M., & Levine, H. (2020). Exploration of the functionality of sugars in cake-baking, and effects on cake quality. *Critical Reviews in Food Science and Nutrition, 61*(2), 283–311.

Sudha, M. L., Baskaran, V., & Leelavathi, K. (2007). Apple pomace as a source of dietary fiber and polyphenols and its effect on the rheological characteristics and cake making. *Food Chemistry, 104*(2), 686–692.

Takahashi, K., Kurose, K., Okazaki, E., & Osako, K. (2016). Effect of various protease inhibitors on heat-induced myofibrillar protein degradation and gel-forming ability of red tilefish (*Branchiostegus japonicus*) meat. *LWT - Food Science and Technology, 68*, 717–723.

Vidal, N. P., Picone, G., Goicoechea, E., Laghi, L., Manzanos, M. J., Danesi, F., … Guillén, M. D. (2016). Metabolite release and protein hydrolysis during the in vitro digestion of cooked sea bass fillets. A study by ^{1}H NMR. *Food Research International, 88*, 293–301.

Wilderjans, E., Luyts, A., Brijs, K., & Delcour, J. A. (2013). Ingredient functionality in batter type cake making. *Trends in Food Science & Technology, 30*(1), 6–15.

Wu, P., Dhital, S., Williams, B. A., Chen, X. D., & Gidley, M. J. (2016). Rheological and microstructural properties of porcine gastric digesta and diets containing pectin or mango powder. *Carbohydrate Polymers, 148*, 216–226.

Xu, S.-S., Liu, Q.-M., Xiao, A.-F., Maleki, S. J., Alcocer, M., Gao, Y.-Y., … Liu, G.-M. (2017). *Eucheuma cottonii* sulfated oligosaccharides decrease food allergic responses in animal models by up-regulating regulatory t (Treg) Cells. *Journal of Agricultural and Food Chemistry, 65*(15), 3212–3222.

Yang, D., Gao, S., & Yang, H. (2020). Effects of sucrose addition on the rheology and structure of iota-carrageenan. *Food Hydrocolloids, 99*, 105317. https://doi.org/10.1016/j.foodhyd.2019.105317.

Yang, D., & Yang, H. (2020). The temperature dependent extraction of polysaccharides from eucheuma and the rheological synergistic effect in their mixtures with kappa carrageenan. *LWT - Food Science and Technology, 129*, 109515. https://doi.org/10.1016/j.lwt.2020.109515.

Zhao, L., Zhao, X., Wu, Ji'en, Lou, X., & Yang, H. (2019). Comparison of metabolic response between the planktonic and air-dried *Escherichia coli* to electrolysed water combined with ultrasound by ^{1}H NMR spectroscopy. *Food Research International, 125*, 108607. https://doi.org/10.1016/j.foodres.2019.108607.

Zhao, X., Chen, L., Wu, Ji'en, He, Y., & Yang, H. (2020). Elucidating antimicrobial mechanism of nisin and grape seed extract against *Listeria monocytogenes* in broth and on shrimp through NMR-based metabolomics approach. *International Journal of Food Microbiology, 319*, 108494. https://doi.org/10.1016/j.ijfoodmicro.2019.108494.

Zhu, Y., Hsu, W. H., & Hollis, J. H. (2013). The impact of food viscosity on eating rate, subjective appetite, glycemic response and gastric emptying rate. *PloS One, 8*(6), e67482.